Derived Input Function from Dynamic Cardiac ^{18}F-FDG PET Images in Rodents based on the Generalized Gaussian ICA Model

R. Mabrouk[1,2], S. Prevost[2], F. Dubeau[3], and L. Bentabet[4]

[1]Department of Computer Sciences Université de Sherbrooke (Qc) Canada, [2]Department of Nuclear Medicine and Radiobiology Université de Sherbrooke (Qc) Canada, [3]Department of Mathematics Université de Sherbrooke (Qc), Canada and [4]Department of Computer Science, Bishop's University, Sherbrooke (Qc), Canada

Abstract—**The aim of this study is to develop a new method to extract input function (IF) from dynamic positron emission tomography (PET) data using the well known [^{18}F]-2-Deoxy-2-fluoro-d-glucose (^{18}F-FDG) for the determination of the myocardial metabolic rate of glucose (MMRG). In the case of cardiac studies, the IF can be obtained directly from the data by mean of a region of interest (ROI) drawn over the blood pool. However, in small animal imaging, hearts and arteries are small compared to the scanner spatial resolution. Consequently, vascular radioactivity is spilled over adjacent tissues and vice versa. As a result, curves obtained from ROIs are made up of a mixture of clean blood activity and the surrounding tissues activities.**

In this work, we assume that the elementary activities of the ventricular blood pool and the myocardium are spatially independent and that dynamic PET image frames are composed of a mixture of them. We use the independent component analysis (ICA) and a Generalized Gaussian Distribution (GGD) model in order to reveal the unknown de-mixing matrix. The derived ICA-IF are then compared to IF derived from invasive arterial blood samples. Results display similar shapes to those obtained by arterial sampling. Moreover, the MMRG calculated using the ICA-IF and two-compartment model correlated well with the results obtained from the sampled IF (2% difference only).

Keywords: PET, Kinetic Modeling, Input Function, independent component analysis.

INTRODUCTION

Using PET, the kinetics of an injected radiotracer can be represented as a spatial distribution of radioactivity. Afterward, two-compartment model is often used to describe relationships between the radioactivity in the blood and in target organs. It aims to assess metabolic process such as the rate of glucose consumption in the case ^{18}F-FDG tracer. [1]

This model uses measured images and requires necessarily an input function (IF). Nowadays, the gold standard to obtain IF's remains the invasive arterial plasma sampling procedure. However, the latter approach may cause physiological perturbation in small animals and thus represent a drawback.

To overcome this limit, alternate methods are suggested to estimate IF from images. Two of these methods particularly estimate the left ventricular time activity curve from actual dynamic cardiac PET images: factor analysis and independent component analysis. The factor analysis of dynamic structures (FADS) method can estimate IF, but it requires additional anatomical assumptions to address the non-uniqueness problem [1]. ICA appears to be a more attractive approach, because it can extract IF without any anatomical assumption [2-5]. Since the first ICA solution to blind source separation is introduced, many methods were developed such as mutual information minimization, maximum likelihood estimation, FastICA among others [6]. The major common point for these algorithms is the assumption of a Gaussianity of observations and the non-Gaussianity of sources. These algorithms are generally reliable to extract sources from brain PET images due to the low volume of blood in the organ. However, in the case of cardiac dynamic images, where blood source density can be assumed as a sub-Gaussian due to the uniformity of blood, and tissue source density can be assumed as a super-Gaussian due to its heterogeneity, those algorithms can fail.

In the present paper, we introduce an approach based on Generalized Gaussian Distribution (GGD) ICA to extract IF from ^{18}F-FDG PET images. The hypothesis we make is based on a priori information, which provides that the two sources have a sub-Gaussian (blood) and super-Gaussian (tissue) spatial distributions. Unlike the algorithm EPICA developed by Naganawa *et el* where they used a kurtosis measure to separate sources then extrat IF, in our approach we use the shape parameter to separate sources.

The paper is organized as follows. Section 2 describes the animal preparation and its measurement. In Section 3, data preprocessing and parameter estimation of a GGD and a natural gradient to estimate the separation matrix are explored. In section 4, we present the results of the approach.

I. EXPERIMENT

Experiments were performed on eighteen male Fischer rats of 200g ± 22g. The animals had free access to food and water throughout the study. Forty minutes dynamic acquisitions in list-mode were performed on the Sherbrookes' small animal PET scanner (LabPET4). A venous catheter was installed into the caudal vein for the radiotracer injection. The injection of

Manuscript received february 14, 2012.
Corresponding author: Rostom.mabrouk@usherbrooke.ca.
Department of Computer Sciences Université de Sherbrooke
Sherbrooke, (Qc) Canada.

50 ± 5 MBq of FDG in a volume of 400 µL was done over the course of 1 minute using an automatic infusion pump in the tail vein. A dynamic series of 27 frames were sorted out from the list-mode data, using the following sequence: 12 × 10 sec, 6 × 30 sec, 6 × 150 sec, 2 x 5 min, and a final frame of 10 min. Image slices were reconstructed using the Maximum Likelihood Expectation Maximization (ML-EM) algorithm.
During the acquisition, blood was withdrawn through a femoral artery catheter at 20, 40, 50, 60, 70, 90, 120, 150, 180 sec and at 5, 10, 15, 20, 25, 35 min. The sampled IF were generated from a linear interpolation of the blood sampling data to the PET dynamic series of 27 frames. Thirty minutes after the injection, the glucose level was obtained from the plasma analysis using a commercial reagent kit (Siemens Healthcare Diagnostic Inc., Deerfield, IL, USA) and an automated clinical chemistry analyzer (Dimension Xpand Plus, Siemens Healthcare Diagnostic Inc., IL, USA).

II. METHOD

A. Preprocessing data

Let us consider an ^{18}F-FDG PET measure. This measure is reconstructed into an images sequence of size $t \times M \times N$ pixels. Each pixel of coordinates $(t, m, n) \in [1 \times \tau] \times [1, M] \times [1, N]$ can take I possible gray-level values which indicate the radioactivity emitted by the corresponding site over time. Figure 1 illustrates the linear dynamic heart PET model.

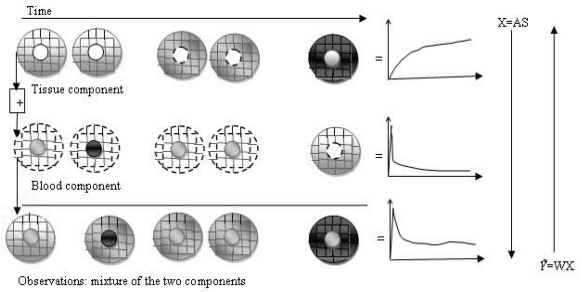


Figure 1- Illustration of the linear dynamic PET model. The FDG is delivered from the blood and then tends to accumulate in tissue. The image sequence is assumed to be a sum of blood component and tissue component when they are statistically independent.

The proposed algorithm attempts to estimate the blood volume image and the tissue volume image to describe accurately the time course of the distribution of the tracer and to provide an IF for the two-compartment model. To reach this goal we arrange the three dimension data into a two dimension Z data. The first dimension is τ which is the time course and the second dimension is $N \times M$ which is the spatial distribution of pixels. In the case of our reconstructed image as described in Section 2, $N = M = 160$. Once we have the mixture observation, the first step is a reduction of a dimension row by applying a PCA and keeping the two spatial components. Thus we obtain:

$$X = AS \tag{1}$$

where X $(2 \times N^2)$ is the principal whitened and centred observation (zero mean and unit variance), S $(2 \times N^2)$ represents the unknown sources, and A (2×2) is an unknown mixing matrix.
Under the assumption that source distributions can be modeled by a GGD, the ICA is able to identify the de-mixing matrix W. Hence we can approximate S by a transformed output $\tilde{S}$ given by:

$$\tilde{S} = WX \tag{2}$$

B. The generalized Gaussian model and its parameter estimation

Among the mathematical models for ICA available in the literature, the GGD is a particularly attractive candidate. It is based on its two main properties: (1) flexibility (statistical behaviors), and (2) the requirement of only one additional parameter compared to the Gaussian model (i.e. it can approximate a large class of statistical distributions)
The analytical equation of the GGD that we adopt in this paper for modeling the two spatial distribution sources is given by:

$$p(\xi; \mu, \sigma, \beta) = \frac{\beta}{2\sigma\Gamma\left(\frac{1}{\beta}\right)} e^{-\left[\frac{|\xi-\mu|}{\sigma}\right]^{\beta}} \tag{3}$$

where μ, σ, β are respectively the mean, the scale and the shape parameters. A common way to estimate the set of statistical parameters consists of maximizing the log likelihood $L(\xi; \mu, \sigma, \beta)$ defined by.

$$L(\xi; \mu, \sigma, \beta) = \sum_{i=1}^{N^2} \log\ p(x_i; \mu, \sigma, \beta) \tag{4}$$

The estimated parameters are obtained by solving the following system:

$$\frac{\partial L}{\partial \mu} = \frac{\partial L}{\partial \beta} = \frac{\partial L}{\partial \sigma} = 0 \tag{5}$$

where

$$\begin{cases} \dfrac{\partial L}{\partial \mu} = \displaystyle\sum_{i=1}^{N^2} -\beta/\sigma^{\beta}\ sign(x_i - \mu)|x_i - \mu|^{\beta-1} \\ \dfrac{\partial L}{\partial \beta} = \displaystyle\sum_{i=1}^{N^2} \left[\frac{1}{\beta} + \frac{1}{\beta^2}\Psi\left(1/\beta\right) - \left(\frac{|x_i - \mu|^{\beta}}{\sigma^{\beta}}\right) \times ln\left(\frac{|x_i - \mu|}{\sigma}\right)\right] \\ \dfrac{\partial L}{\partial \sigma} = -\dfrac{1}{\sigma} + \beta\sigma^{-\beta-1}|x_i - \mu|^{\beta} \end{cases} \tag{6}$$

where $\Psi(.) = \frac{\Gamma'(.)}{\Gamma(.)}$ is the digamma function.

After some simple transformations, we get the estimate of the scale parameter from the following equation [7]:

$$\sigma = \sigma(\mu, \beta) = \left[\beta \times \sum_{i=1}^{N^2} \times |x_i - \mu|^{\beta}\right]^{1/\beta} \quad (7).$$

C. Natural gradient based ICA algorithm

The objective of the GGD-based ICA is to calculate a de-mixing matrix W that maximizes the likelihood of the mixture probability $P(X)$ of the J sources $(J = 2)$. According to equation 2 the likelihood is defined by:

$$L(W) = log \prod_{j=1}^{J} p(X_j) \quad (8)$$

We assume that the j^{th} source is modeled by a GGD whose parameters are estimated as shown previously. The maximum likelihood leads to the following equation:

$$L(W) = log|det(W)| + \sum_{i=1}^{N^2} \log p(\tilde{S}_{j,i}) \quad (9)$$

where $\tilde{S}_j$ represents the GGD function for source j. Let us define the following non-linear function (see [7]).

$$\phi_j(\tilde{S}_j) = \frac{d \log (p(\tilde{S}_j)}{d\tilde{S}_{j_i}} \quad (10)$$

In the case of GGD (equation 3), we have:

$$\phi_j(\tilde{S}_j) = -\beta\alpha^{-\beta} sign(\tilde{S}_j - \mu)|(\tilde{S}_j - \mu)|^{\beta-1} \quad (11)$$

With this definition, the gradient is given by:

$$\nabla L(W) = \frac{\partial L(W)}{\partial w_j} = w_j + \phi_j(\tilde{S}_j) x^T{}_j \quad (12)$$

We use the natural Riemannian gradient (denoted by $\tilde{\nabla} L(W) = \frac{\partial L(W)}{\partial w_j} W^T W$) learning algorithm to calculate W which is given by:

$$w_j(t+1) = w_j(t) - sign(\tilde{\nabla} L(W)) \times \tilde{\nabla} L(W)$$
$$= w_j(t) - sign\left(\tilde{\nabla} L(W)\right) \times \frac{\partial L(W)}{\partial w_j} W^T(t) W(t)$$
$$= w_j(t) + sign\left(I - \phi_j(\tilde{S}_j)\tilde{\tilde{S}}_j^T\right)\left(I - \phi_j(\tilde{S}_j)\tilde{\tilde{S}}_j^T\right) w_j(t) \quad (13)$$

III. RESULTS

Figure 2 shows the last frame of the initial PET image before calibration and illustrates appropriately the contamination effect, which makes it difficult to extract a true activity from the initial data sequence using a mean of the activity calculated from manual ROI drawn over the blood pool. The cross-contamination is due to the organ movements and the limited spatial resolution of the PET scanner.

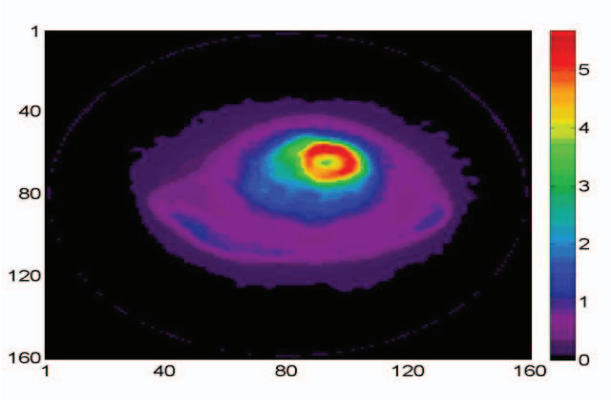


Figure 2- Image of the rat heart measured with ^{18}F-FDG during 10 min at 35 min after tracer injection. The blood pool is contaminated with tissue activity due to the limited spatial resolution of the scanner.

The GGD model ICA allows to produce an accurate spatial pixel separation which generates a blood image volume and a tissue image volume with low cross-contamination. This separation is a result of a good estimation of the separating matrix W. This matrix can separate the two principal time activity curves, which correspond to the IF, and the tissue time activity curve.

Figure 3 (A) shows the whole blood time activity (IF), calculated using manual ROI drawn over the blood pool, and the IF extracted with the GGD model ICA. Figure 3 (B), illustrates a comparison between the sampled IF and the ICA-IF after it was corrected for the plasma activity. The correction is based on application of a factor $R_{BP}(t)$ as follows:

$$IF_P = R_{BP}(t) IF_W, \quad (14)$$

where IF_W is the time activity curve of the whole blood extracted from images and IF_P is the time activity curve of the plasma. R_{BP} is calculated as described in [8], and given by:

$$R_{BP}(t) = 0.386 \exp(-0.191\, t) + 1.165 \quad (15)$$

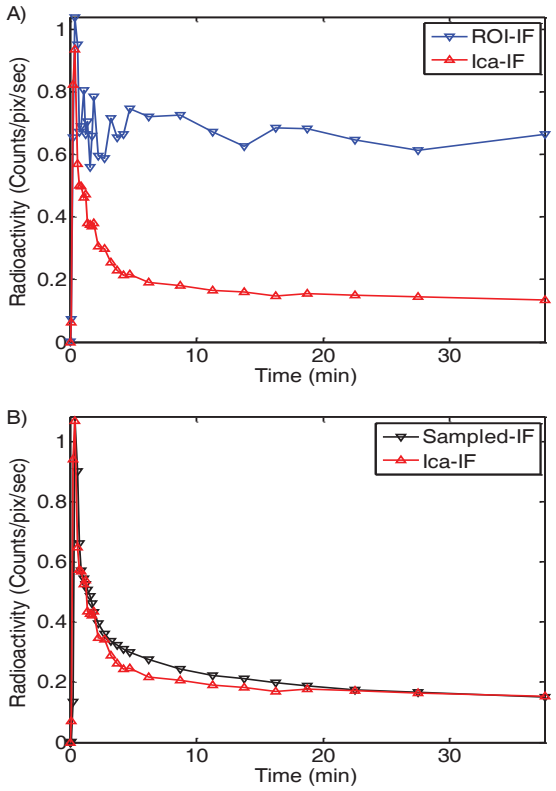


Figure 3- Estimated and plasma sampled input functions from the same rat. (A) Comparison between sampled GGD-ICA IF and IF from ROI shows ROI-IF higher than the ICA-IF, primarily due to spillover from myocardium ^{18}F-FDG activity. (B) Sampled IF and ICA-IF calibrated with a mean of the last three samples are closed

The MMRG values for the eighteen rats are computed separately using sampled IF, the ICA-IF and the ROI-IF. The results are reported as box plots in Figure 4.

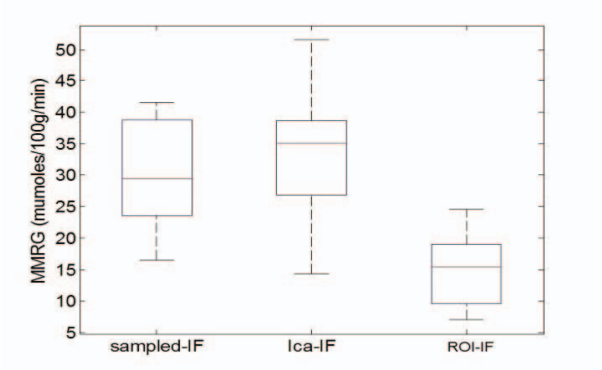


Figure 4- Comparison of ^{18}F-FDG MMRG values obtained with the three methods of analysis. The whisker diagram shows a large highest score and lowest score, which are due to some noised image measures.

The t-test between MMRG calculated with sampled IF and calculated with ICA-IF shows no significant difference ($p<0.05$). On the other hand, the t-test between MMRG calculated with the sampled IF and calculated from the ROI IF shows a significant difference ($p> 0.05$). We can interpret quantitatively the difference existing in the MMRG values by computing relative gap between calculated MMRG. Indeed, the value computed by our method differs by 2% from the gold standard whereas the value computed from ROI-IF differs by 51%.

IV. CONCLUSION

The aim of this research was to solve the separation problem of a mixture of radioactivity signal delivered by two adjoining independent sites (blood and tissue). Our results show that ICA-IF can generate a very good approximation of the IF providing a curve whose shape is similar to the gold standard sampled IF, and importantly, which requires much smaller blood samples. We are currently investigating validation of this method via application of the method to another tracer ^{13}N-Ammonia and 82-Rubidium.

REFERENCES

[1] H.M. Wu, C.K. Hoh, Y. Choi *et al*, "Factor analysis for extraction of blood time-activity curves in dynamic FDG-PET studies," J Nucl Med, vol. 36, pp.1714–1722, 1995.

[2] M. Naganawa, Y. Kimmura, K. Oda, K. Ishiwata, and A. Matani, "Extraction of a plasma time-activity curve from brain PET images based on independent component analysis," IEEE Trans on, Biomed Eng, vol. 52, pp.201–210, 2005.

[3] M. Naganawa, Y. Kimmura, K. Ischii, K. Oda, and K. Ishiwata, "Temporal and special blood information estimation using Bayesian ICA in dynamic cerebral positron emission tomography," IEEE Trans on, Digital Signal Processing, vol. 17, pp.973–993, 2007.

[4] K.H. Su, J.S. Lee, J.H. Li, Y.W. Yang, R.S. Liu, and J. C. Chen, "Partial volume correction of the microPET blood input function using ensemble learning independent component analysis," Phys Med Biol, vol. 54, pp.1823–1846, 2009.

[5] M.M. Mendez, A. Juslin, V.S. Nesterov, K. Kalliokoski, J, Knuuti, and U. Ruotsalaine, "ICA Based Automatic Segmentation of Dynamic H215O Cardiac PET Images," IEEE Inform tech in Biomed, vol. 14, pp.795–802, 2010.

[6] A. Hyvärinen and E. Oja., "Independent Component Analysis: Algorithms and Application," Neural Networks, vol. 13, pp. 411–430, 2000.

[7] S. Amiri, A.Cichocki, and H.H. Yang, "A New Learning Algorithm for Blind Source Separation," In Advances in Neural Information Processing Systems, vol. 8, pp.757–763, 1996.

[8] H.M. Wu, S. Guodong, C. Lee, *et al*, "Mouse plasma and whole blood difference in 2-[^{18}F] fluoro-2-deoxy-D-glucose (^{18}F-FDG) concentration: implication for quantitative mouse 18F-FDG PET studies," J Nucl Med, vol. 48, pp.837–845, 2007.